2022

Transient Oil-refrigerant Mixture Migration and Change of Properties at Compressor Shutdown

Xin Wang

Syed Angkan Haider

Pega Hrnjak

Stefan Elbel

Transient Oil-refrigerant Mixture Migration and Change of Properties at Compressor Shutdown

Xin WANG[1], Syed Angkan HAIDER[1], Pega HRNJAK[1,2], Stefan ELBEL[1,2]*

[1]Air Conditioning and Refrigeration Center, Department of Mechanical Science and Engineering, University of Illinois at Urbana-Champaign, 1206 West Green Street, Urbana, IL 61801, USA

[2]Creative Thermal Solutions, Inc., 2209 North Willow Road, Urbana, IL 61802, USA

* Corresponding Author: elbel@illinois.edu

ABSTRACT

The oil migration has great impact on the vapor compression systems, especially for systems that require frequent on-off cycling. Excessive amount of oil retained in the system and lack of oil return to the compressor can cause low system efficiency and potential compressor failure. This paper aims at exploring oil-refrigerant mixture properties during startup and shutdown period at different locations in the system. The variation of temperature and pressure would result in different mixture concentrations and properties. Oil properties like solubility, viscosity, density, surface tension and contact angle can be influenced and will affect system performance.

During the compressor shutdown, the oil flow in contact with the inner wall of discharge stops immediately with while oil droplets in the vapor core flow slower and stop gradually. In the end, oil droplets flow down and coalesce with oil film to accumulate at the bottom of the tube. The high-speed camera and video analysis method are used to analyze oil migration and show variation of surface tension, viscosity, and wettability. Properties of mixture like solubility, density, saturation pressure and viscosity are predicted using existing models.

1. INTRODUCTION

Lubricant is essential in vapor compression systems. To keep compressor working properly, oil is required to reduce friction and minimize wear inside the compressor. Oil properties are supposed to meet the lubrication demand suitably. During compressor shutdown, refrigerant migrates to components with the lowest temperature in the system. Vapor refrigerant is dissolved into liquid oil and significantly changes oil properties such as density, viscosity, saturation pressure and surface tension. Too much refrigerant in oil can decrease magnitude of oil viscosity, which is one of the most important factors in compressor performance. Large solubility change at startup can cause serious problems like oil foaming, lack of lubrication, etc. Many studies mostly focus on oil properties at steady state under different system working conditions. For decades, measurement of refrigerant-oil mixture properties has been investigated. Daniel *et al*. (1982) established chart for dilution and viscosity variations under the system operating temperature and pressure. Seeton and Hrnjak (2006) measured mixture properties with viscosity meter and sampling method based on ASTM Standard D445, and improved Daniel chart with more refrigerant and lubricant combinations in different temperature and pressure ranges. In addition, researchers developed property estimation model based on temperature, pressure, and refrigerant mass fraction variation. Yokozeki (1994) developed general solubility and viscosity model of refrigerant-oil mixture based on thermodynamic property experimental data. Seeton and Hrnjak (2009) modeled vapor-liquid-equilibrium (VLE) and vapor-liquid-liquid-equilibrium (VLLE) properties of CO_2-lubricant mixtures based on ASTM Standard D7142.

Unfortunately, there have not been many previous studies on thermophysical property changes and transient migration of oil-refrigerant mixture at startup and shutdown. The refrigerant dissolves after shutdown and escapes from oil at startup. To illuminate the mixture vapor-liquid equilibrium (VLE) behavior effect on mixture properties under saturation process, this study modeled solubility, density, viscosity and saturation pressure variation at startup and shutdown. Furthermore, oil migration at compressor suction and discharge is analyzed and discussed. Oil and refrigerant flow behavior shows close relation to surface tension and viscosity change.

2. EXPERIMENT DESCRIPTION

The schematic diagram of the experimental apparatus is shown in Figure 1. The main components of the system are variable-speed electrical scroll compressor, microchannel-type evaporator and condenser, and an electronic expansion valve (EEV). Flow visualization setup is built at compressor discharge and suction. Two environmental chambers are controlled at the AHRI A_{Full} conditions as prescribed in AHRI standard 210/240 (2017) with heaters and cooling chiller. R134a and polyalkylene glycol (ISO PAG 46) lubricating oil are used as refrigerant and lubricant for the experiment. This is a commonly used combination and is fully miscible in the system under the working conditions according to Seeton and Hrnjak (2009). Basic lubricant properties are shown in Table 1.

Table 1: Basic properties of ISO PAG 46 (ND-8)

Density (g/cc)	**Viscosity at 40**°C	**Viscosity at 100**°C	**Flash point**
0.9944	43.32 cSt	9.234 cSt	204°C

The steady-state data for 2000 RPM is shown in Table 2. The temperature and pressure at compressor suction and discharge are measured with T-type thermocouples and pressure transducers to estimate the mixture composition and property change.

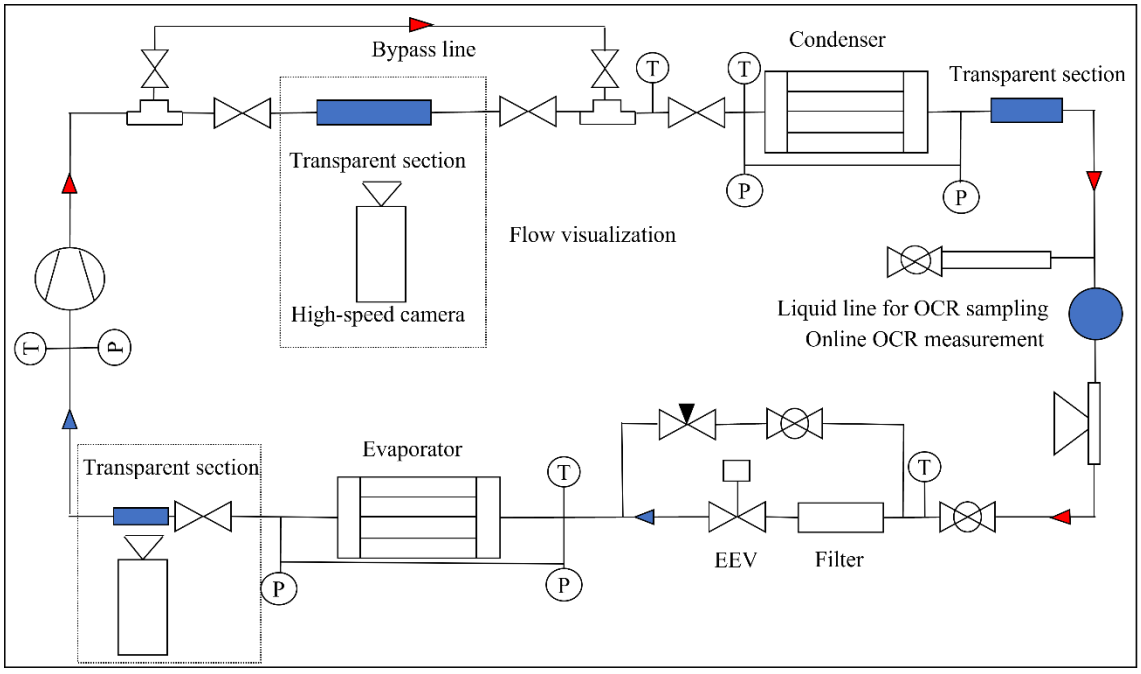

Figure 1: Schematic of the test facility

The flow visualization section is composed of a high-speed camera, LED panel light source and transparent tube. The detailed tube material and sizes are discussed in the works of Wang *et al.* (2022). Visualization position of discharge is 0.8 m downstream of the compressor. Visualization position of suction is 0.5 m downstream of the compressor.

Table 2: Steady state data for 2000 RPM

Subcooling (°C)	**Superheat (°C)**	**Suction pressure (kPa)**	**Suction temperature (°C)**	**Discharge pressure (kPa)**	**Discharge temperature (°C)**
6	10.5	445	25.5	1110	66.6

3. PROPERTY MODELING

This section introduces existing models which will be used to estimate refrigerant solubility in oil and mixture properties.

3.1 Refrigerant-oil Mixture Solubility Model

Solubility of refrigerant in oil can cause significant deviations between the thermodynamic properties of refrigerant-oil mixture and pure oil. Many refrigerant-oil solubility models based on vapor liquid equilibrium are available in the literature. Among them, Martz *et al.* (1996) presented that the liquid-vapor phase fugacity (gamma-phi) model is commonly used in predicting mole fraction of refrigerant in liquid phase. To calculate coefficients in the model, semi-theoretical mixture models such as Flory-Huggins Polymer Theory, Wilson Model, non-random two-liquid model (NRTL), Universal Quasichemical Model (UNIQUAC), and Heil Model are applied based on experimental data. However, these models need adequate thermodynamic property data of different refrigerant-oil mixtures. The reliability of vapor pressure and temperature correlation varies among different mixture concentrations. Greber and Crawford (1992) found strong negative deviations between Flory-Huggins Polymer Theory solution and experimental results. To improve accuracy of solution prediction and simplify calculation, here, an empirical model of R134a-PAG oil solubility presented by Greber and Crawford (1992) is applied to predict refrigerant mass fraction. The temperature-pressure-concentration relation is given by the Equation (1) to (4):

$$T^* = (1 - w_r)[A(w_r) - B(w_r)p] \tag{1}$$

Where

$$T^* = \frac{T - T_{sat}(p)}{T_{sat}(p)} \tag{2}$$

$$A(w_r) = a_0 + \frac{a_1}{{w_r}^{1/2}} \tag{3}$$

$$B(w_r) = b_0 + \frac{b_1}{{\omega_r}^{1/2}} + \frac{b_2}{\omega_r} + \frac{b_3}{{\omega_r}^{3/2}} + \frac{b_4}{{\omega_r}^2} \tag{4}$$

p = system pressure, Pa
T = temperature, K
ω_r = refrigerant mass fraction
T_{sat} = saturation temperature at system pressure, K
a_0 through b_4: empirical correlation constants

Table 3: Values of empirical coefficients for R134a-PAG mixture

Coefficient	a_0	a_1	b_0	b_1	b_2	b_3	b_4
R134a/PAG	-7.15E-2	5.99E-2	1.71E-3	-2.97E-3	1.70E-3	-3.76E-4	3.00E-5

Values of empirical coefficients used in the Equation (3) and (4) are shown in Table 3. The model can be used to predict liquid refrigerant fraction with temperature and system pressure. However, there are limitations of the model. The model is not capable of predicting solubility when the refrigerant is in two-phase, also not accurate at high refrigerant concentrations. In this paper, this model is mostly used in low refrigerant concentrations conditions with superheated refrigerant.

3.2 Mixture Liquid Density

Mixture liquid density can be calculated with given temperature and refrigerant mass fraction. The empirical equation is supposed by Seeton and Hrnjak (2009) as below:

$$\rho = a_1 + a_2 T + a_3 T^2 + \omega_r(a_4 + a_5 T + a_6 T^2) + {\omega_r}^n(a_7 + a_8 T + a_9 T^2) \tag{5}$$

Where

$\rho =$ density, g/cc
$T =$ temperature, K
$\omega =$ refrigerant mass fraction
$n =$ concentration coefficient
$a_1$through a_9: correlation constants

$a_1$through a_9 empirical values are provided in Table 4 to predict density of R134a (0-70%)-PAG 46 mixture from Seeton and Hrnjak (2006).

Table 4: Values of empirical coefficients for R134a-PAG mixture density

Coefficient	a_1	a_2	a_3	a_4	a_5	a_6	a_7	a_8	a_9	n
Density R134a/PAG (0 to 70% R134a)	1.23	-8.81E-4	6.00E-8	5.91E-1	-1.86E-3	2.63E-6	1.18E-1	9.92E-4	-4.96E-6	2

.

3.3 Mixture Liquid Viscosity

Mixture liquid viscosity can be calculated with given temperature and refrigerant mass fraction. The empirical equation is supposed by Seeton and Hrnjak (2009):

$$\ln\left(\ln\left(\upsilon_{mix}+0.7+e^{-\upsilon_{mix}}K_0(\upsilon_{mix}+1.244067)\right)\right)=\sum_I\left(\left(1+\sum_j\varphi_{ij}\omega_i\omega_j\right)*\omega_i*(A_i-B_i\ln(T))\right) \quad (6)$$

Where
$T =$ temperature, K
$\omega_i =$mass fraction of component i
$\upsilon_{mix} =$mixture kinematic viscosity, cSt
A_i and B_i: fit parameters for each pure fluid in the mixture
K_0: zero order modified Bessel function of the second kind
$\varphi_{ii}=\varphi_{jj}=0$
$\varphi_{ij}=A_{ij}+B_{ij}\omega_i+C_{ij}T+D_{ij}\omega_i T$

Table 5: Kinematic viscosity parameters of R134a-PAG mixture

		ISO PAG 46	R-134a
Viscosity parameters	A	17.789	19.146
	B	2.866	3.84
Interaction Parameters	A_{ij}	8.9211	-21.0421
	B_{ij}	-0.0208	0.0348
	C_{ij}	-17.6611	19.2536
	D_{ij}	16.2445	-9.8310

3.4 Mixture Saturation Pressure

Mixture saturation pressure can be estimated with given temperature and refrigerant mass fraction. The empirical equation is presented by Seeton and Hrnjak (2009):

$$\log_{10}(P_{mix})=a_1+\frac{a_2}{T}+\frac{a_3}{T^2}+\log_{10}(\omega)\left(a_4+\frac{a_5}{T}+\frac{a_6}{T^2}\right)+\log_{10}^n(\omega)\left(a_7+\frac{a_8}{T}+\frac{a_9}{T^2}\right) \quad (7)$$

Where
$P_{mix} =$saturation pressure, bar

T = temperature, K
ω = refrigerant mass fraction
n = concentration coefficient
a_1 through a_9: correlation constants

Table 6: Values of empirical coefficients for R134a-PAG mixture

Coefficient	a_1	a_2	a_3	a_4	a_5	a_6	a_7	a_8	a_9	n
Mixture vapor pressure	4.19	-8.74E2	-3.95E4	-1.61	7.66E2	-9.14E4	-9.83E-1	1.64E2	-1.68E4	2

4. FLOW VISUALIZATION AND PROPERTY CHANGE AT SUCTION

4.1 Mixture Flow at Suction: Shutdown

Flow visualization at suction during the compressor shutdown is shown in Figure 2. The mixture flow before shutdown was composed of oil annular mist flow and vapor refrigerant flow. 0.23 s after shutdown as Figure 2 (b) shows, the oil film flow stopped. Viscous oil layer distributed uniformly on the tube inner wall. Then after 0.24 s, the oil layer flowed down due to gravity and accumulated at the bottom of the tube as shown in Figure 2 (c), the oil layer was still wavy because of moving vapor refrigerant flow. Finally, 1s after shutdown, oil stopped completely and kept still.

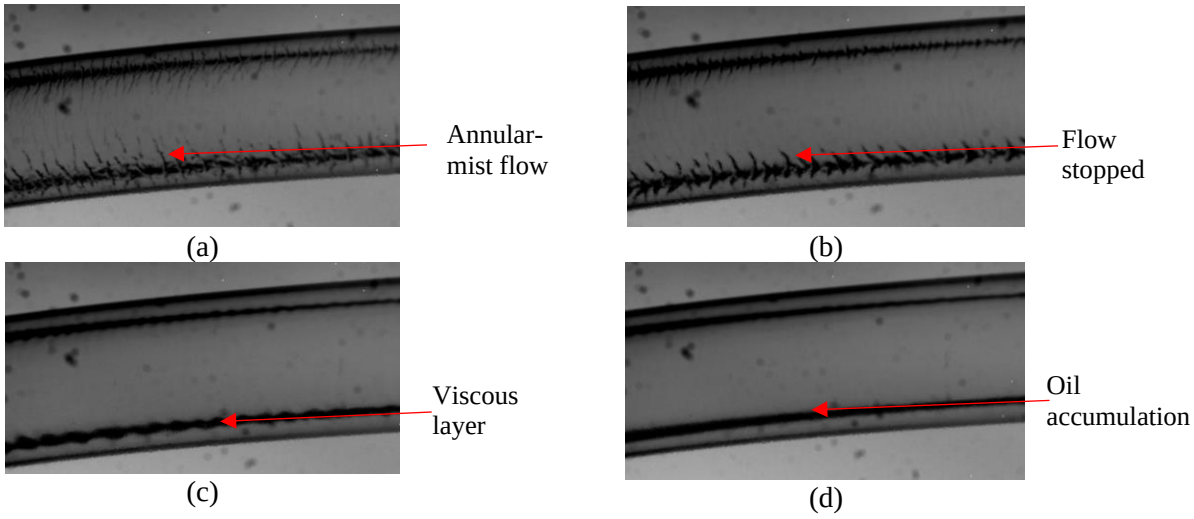

Figure 2: Flow visualization at suction (a) before shutdown (b) 0.23 s after shutdown (c) 0.47 s after shutdown (d) 1 s after shutdown

The flow visualization shows the oil stops flowing. The annular oil film stopped moving forward and spread on the tube wall, then flowed down and stayed steady. During the process, the surface tension and viscosity changed rapidly due to the change of solubility and pressure.

4.2 Mixture Solubility and Saturation Pressure Variation at Suction

Refrigerant solubility in oil is shown in Figure 3 (a). The refrigerant mass fraction is estimated by empirical model discussed in **Section 3.1**. As shown in Figure 3 (a), the solubility dropped rapidly at compressor startup and reached the minimum value of refrigerant mass fraction in liquid phase, which validated phase transaction and oil foam phenomenon for cold startup visualization (Wang *et al.*, 2022). The refrigerant mass fraction maintained at 0.215 at steady state. After shutdown, the solubility increased fast (45s) as suction pressure suddenly increased. Here pressure and temperature have opposite impact on solubility change. The solubility increases with increasing pressure and decreasing temperature according to Henry's Law. The suction temperature increased from 23.6 °C to 25.5 °C (0.6%)

after shutdown, however, the pressure increased from 411.2 kPa to 677.5 kPa (164.8%), which is much more rapidly than thermodynamically change.

The mixture saturation pressure calculated in **Section 3.4** was influenced by refrigerant mass fraction and temperature as shown in Figure 3 (b). The variation trend was like mass fraction. The saturation pressure decreased acutely at startup since large amount of refrigerant escaped from the liquid phase. After shutdown, vapor refrigerant dissolved in oil and gradually condensed to liquid phase, and as a result, the mixture saturation pressure increased.

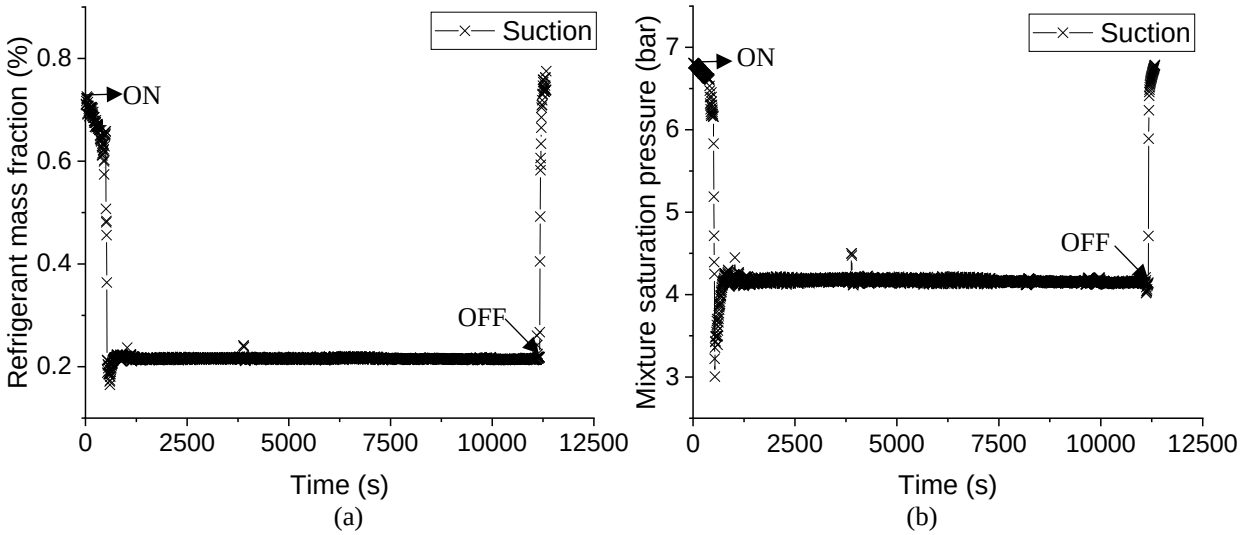

Figure 3: Refrigerant mass fraction (a) and mixture saturation pressure change (b) at suction

4.3 Mixture Density and Viscosity Variation at Suction

Density variation of R134a-PAG 46 mixture calculated by Equation (5) is shown in Figure 4 (a). The density decreased to the minimum value initially, then increased to steady value. During shutdown, the density increased rapidly with increasing refrigerant mass fraction because of higher density of refrigerant than oil.

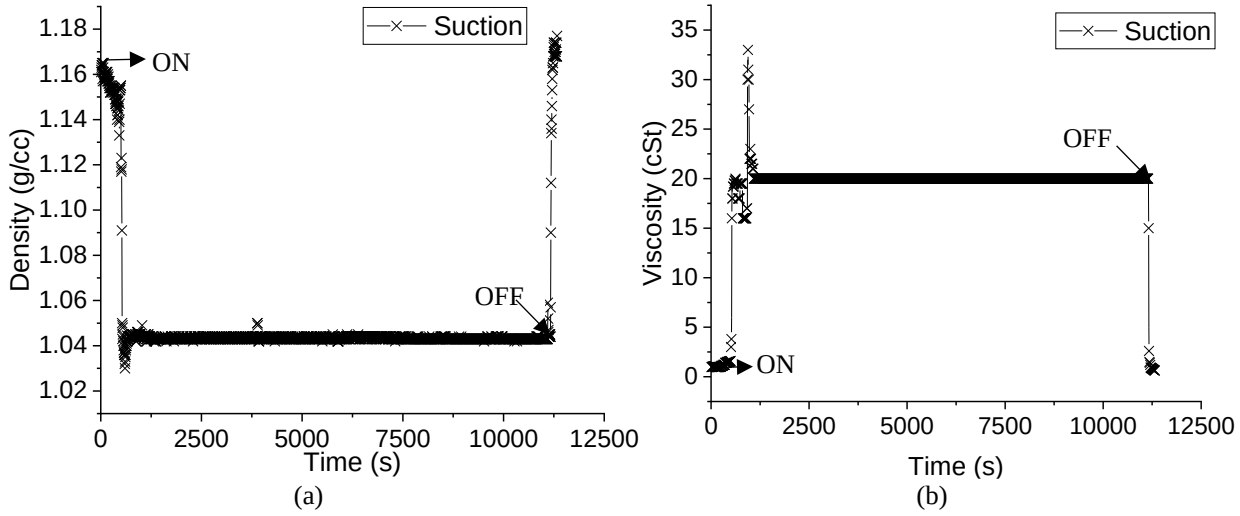

Figure 4: Mixture density (a) and viscosity (b) change at suction

Mixture viscosity change is predicted by Equation (6) and shown in Figure 4 (b). The viscosity increased initially at startup due to refrigerant fraction and temperature decrease. Then three minutes after startup, the suction temperature suddenly decreased from 24 °C to 14 °C, viscosity also showed fluctuation from 18 cSt to 33 cSt at the same time. The viscosity of mixture fixed at 20 cSt at steady state. After shutdown, the viscosity rapidly decreased. As shown in

Figure 3 (a), the solubility increased from 0.2 % to 0.7 % fast after shutdown. In addition, temperature increased 0.6 %. Therefore, viscosity decreased from 20 cSt to 1 cSt in one minute.

5. FLOW VISUALIZATION AND PROPERTY CHANGE AT DISCHARGE

5.1 Mixture Flow Visualization at Discharge: Shutdown

Flow visualization at discharge during compressor shutdown is shown in Figure 5. Before shutdown, as shown in Figure 5 (a), the oil flow was composed of small oil droplets in vapor core as well as oil streams and droplets attached to the inner wall of the tube. The oil droplets in vapor core were more than 2 orders of magnitude faster than oil streams attached to the wall. Due to low oil circulation ratio (OCR) and low compressor speed, the oil was not able to form uniform oil film in the tube wall.

0.78 s after shutdown as shown in Figure 5 (b), the oil stream stopped and dispersed into oil droplets, while the oil droplet was still traveling due to the much higher velocity. After 0.1 s, oil mist stopped traveling with vapor refrigerant and coalesced into oil droplets as shown in Figure 5 (c). The droplets flowed down due to gravity slowly then as shown in Figure 5 (d).

The droplets showed the "tear-like" phenomenon during shutdown in Figure 5. The same phenomenon was observed by Worsoe-Schmidt (1960) and explained with surface tension effect. In addition, Manwell and Bergles (1990) argued oil viscosity change contributed more to "tearing" at the temperature range (0-40 °C). Wongwises *et al.* (2002) believed the tear flowing process might be related to the mixture viscosity and wettability. The wettability (contact angle) of Perfluoroalkoxy alkane (PFA) surface with R134a-PAG 46 mixture is not measured or evaluated before. As a reference, Fukuta *et al.* (2020) evaluated wettability of metal surfaces with refrigerant-oil mixture by measuring the contact angle of mixture, it is found that the contact angle of mixture decreases with increasing refrigerant concentration. But the spread speed of droplets was influenced by tube material because of different solid surface energy.

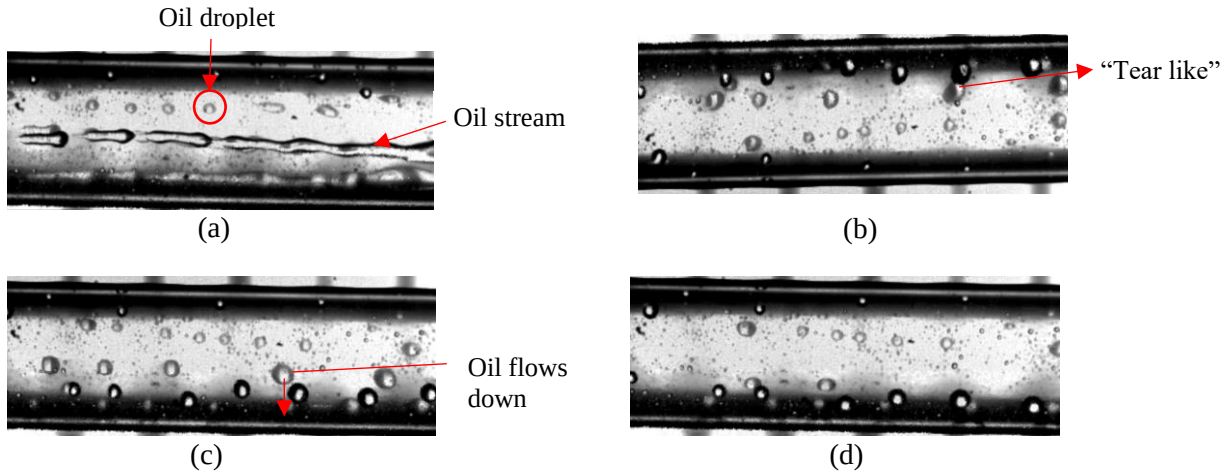

Figure 5: Flow visualization at suction (a) before shutdown (b) 0.78 s after shutdown (c) 0.88 s after shutdown (d) 3.29 s after shutdown

5.2 Mixture Solubility and Saturation Pressure Variation at Discharge

As shown in Figure 6 (a) the refrigerant solubility in oil initially decreased after startup, then suddenly increased to a maximum value of mass fraction then decreased rapidly. Temperature and pressure both decreased in the first three minutes then increased during startup period. The solubility variation was influenced more by pressure at first, because the pressure decreased more rapidly (43 kPa) in the first three minutes after startup. Though the pressure increased, however, it is believed the increasing temperature affected solubility dominantly in the long term, which can explain the decrease of solubility.

Figure 6 (b) shows mixture saturation pressure change. In this case, the saturation pressure showed the same variation trend as the discharge temperature. Although refrigerant mass fraction generally decreased during operation, the saturation pressure still increased because of increasing temperature.

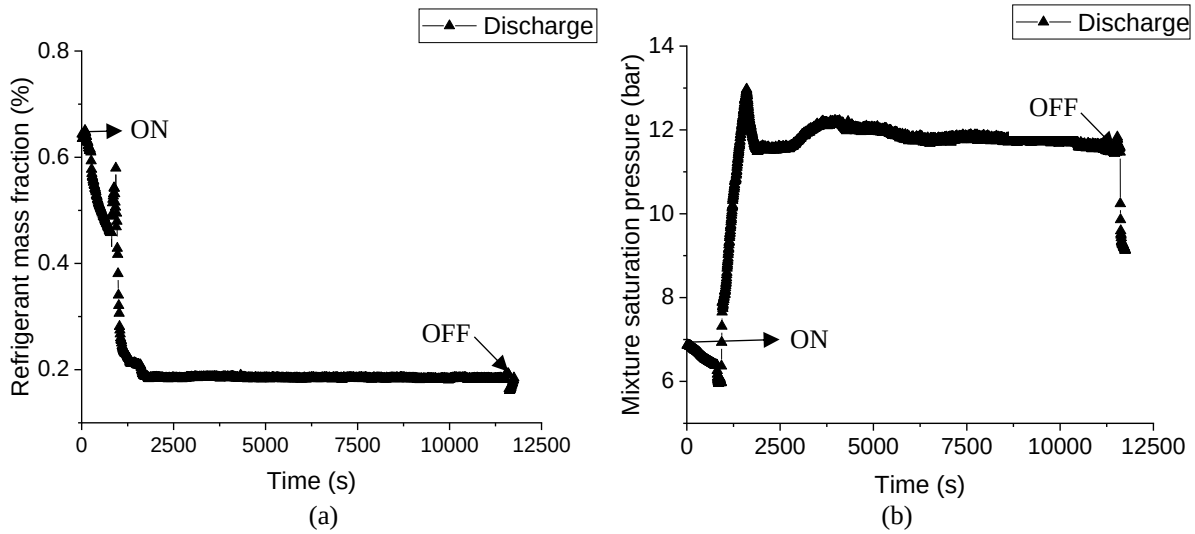

Figure 6: Refrigerant mass fraction and mixture saturation change at discharge (a) Refrigerant mass fraction in liquid (b) Mixture saturation pressure

5.3 Mixture Density and Viscosity Variation at Discharge

Density variation of R134a-PAG 46 mixture is shown in Figure 7 (a). The density decreased initially, then increased to a peak value, then decreased to steady-state value. During shutdown, the density increased slightly due to the slight change of solubility in Figure 6 (a) and temperature.

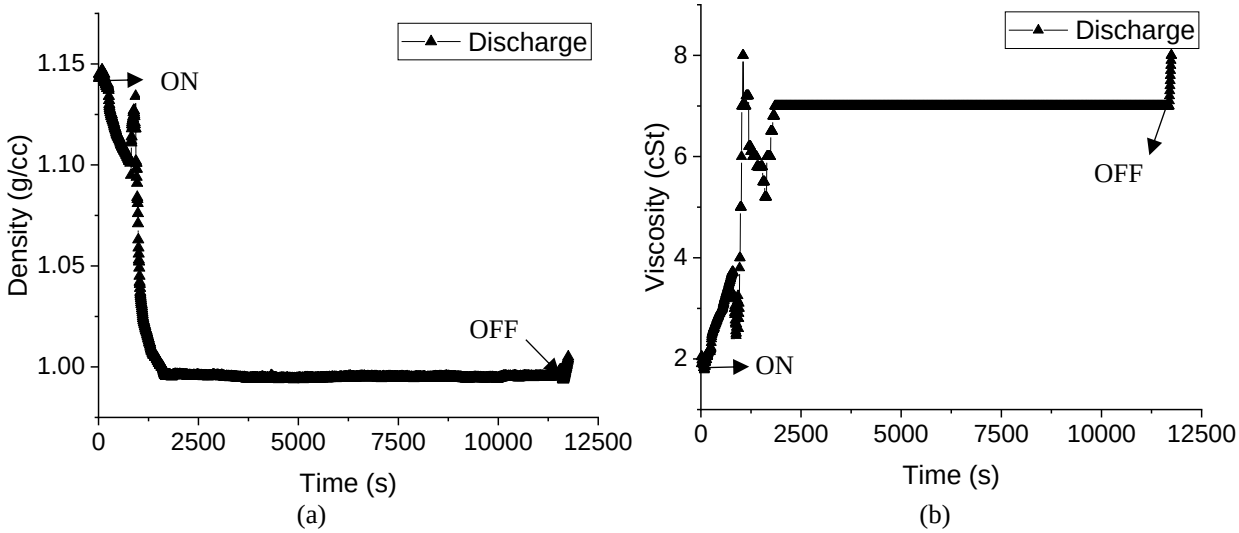

Figure 7: Mixture density (a) and viscosity (b) change at discharge

Mixture viscosity change is predicted by Equation (6) and shown in Figure 7 (b). The viscosity increased initially at startup due to refrigerant fraction decrease. The viscosity of mixture decreases with increasing temperature under at the same concentration. During the first three minutes the solubility decrease was more acute than temperature increase. While 5 minutes after startup, the solubility decrease was slower, and temperature increase effect caused viscosity fluctuation. The viscosity of mixture maintained at 7 cSt at steady state. After shutdown, the viscosity increased slightly because of temperature decrease. Compared to the mixture of viscosity at suction at steady state,

the mixture viscosity at discharge is smaller with the similar refrigerant mass fraction, which is due to the higher temperature (65 °C) at discharge than suction (23 °C).

6. CONCLUSIONS

In vapor compression system, the lubricant oil is essential in increasing the compressor longevity and system performance. The solubility of R134a in ISO PAG 46 oil is modeled with temperature and pressure variations at compressor suction and discharge, which helps understand the mixture behavior and contribute to keep high-quality lubricant in the compressor. The solubility decreased 69% from system off to steady state at suction and decreased 71% at discharge during startup. Properties such as density, saturation pressure, and viscosity are predicted by refrigerant mass fraction, temperature, and pressure. Oil properties changed dramatically due to the temperature and refrigerant concentration change. The viscosity of mixture increased from 1 cSt to 20 cSt at suction during startup and also decreased rapidly after shutdown. At discharge, the viscosity variation shows different effect of solubility and temperature. The flow visualization results at suction and discharge during shutdown show the change of mixture viscosity, surface tension and wettability.

NOMENCLATURE

Ai	coefficient of mixture viscosity	
Aij	coefficient of mixture viscosity	
A(ω_r)	coefficient of solubility	
a_0 through a_9	coefficients	
Bi	coefficient of mixture viscosity	
Bij	coefficient of mixture viscosity	
B(ω_r)	coefficient of solubility	
b_0 through b_4	coefficients of solubility	
Cij	coefficient of mixture viscosity	
Dij	coefficient of mixture viscosity	
OCR	oil circulation ratio	
p	pressure	(kPa)
T	temperature	(K)
ν	kinematic viscosity	(cSt)
φ	coefficient of mixture viscosity	
ρ	density	(g/cc)
ω	mass fraction of component in refrigerant-oil mixture	
Subscript		
*	non-dimensional saturation temperature	
i	component i in refrigerant-oil mixture	
j	component j in refrigerant-oil mixture	
mix	refrigerant-oil mixture	
r	refrigerant	
sat	saturation	

REFERENCES

ASTM Standard D445. (2006). "Standard Test Method for Kinematic Viscosity of Transparent and Opaque Liquids (and Calculation of Dynamic Viscosity)." ASTM International. West Conshohocken, PA. 2006. DOI: 10.1520/D0445-06.www.astm.org.

ASTM Standard D7152. (2005el). "Standard Practice for Calculating Viscosity of a Blend of Petroleum Products." ASTM International. West Conshohocken, PA. 2005. DOI: 10.1520/D7152-05E01 www.astm.org.

Daniel, G., Anderson, M. J., Schmid, W., & Tokumitsu, M. (1982). Performance of selected synthetic lubricants in industrial heat pumps. Journal of Heat Recovery Systems, 2(4), 359-368.

Fukuta, M., Sumiyama, J., Motozawa, M., & Chaiworapuek, W. (2020). Wettability of metal surface with oil/refrigerant mixture. International Journal of Refrigeration, 119, 131-138.

Grebner, J. J. (1992). The effects of oil on the thermodynamic properties of dichlorodifluoromethane (R-12) and tetrafluoroethane (R-134a). Air Conditioning and Refrigeration Center. College of Engineering. University of Illinois at Urbana-Champaign..

Manwell, S. P. (1990). Gas-Liquid Flow Patterns in Refrigerant Oil Mixtures. ASHRAE transactions, 96, 456-464.

Martz, W. L., Burton, C. M., & Jacobi, A. M. (1996). Vapor-liquid equilibria for R-22, R-134a, R-125, and R-32/125 with a polyol ester lubricant: measurements and departure from ideality (No. CONF-960254-). American Society of Heating, Refrigerating and Air-Conditioning Engineers, Inc., Atlanta, GA (United States).

Seeton, C. J., & Hrnjak, P. (2006). Thermophysical properties of CO2-lubricant mixtures and their effect on 2-phase flow in small channels (less than 1mm).

Seeton, C. J., & Hrnjak, P. S. (2009). CO2-lubricant two-phase flow patterns in small horizontal wetted wall channels: The effects of refrigerant/lubricant thermophysical properties. Urbana.

Wang, X., Haider, S. A., Hrnjak, P., & Elbel, S. (2022). Transient migration of oil at compressor discharge and suction during startup. *Proceedings of the International Refrigeration and Air Conditioning Conference*, Paper 2266, West Lafayette, IN, USA (manuscript submitted)

Wongwises, S., Wongchang, T., Kaewon, J., & Wang, C. C. (2002). A visual study of two-phase flow patterns of HFC-134a and lubricant oil mixtures. Heat Transfer Engineering, 23(4), 13-22.

Worsoe-Schmidt, P. (1960). Some Characteristics of Flow Pattern and Heat Transfer of Fren 12 Evaporation in Horizontal Tubes. *The J of Refrigeration*, *3*(2), 40-44.

Yokozeki, A. M. (1994). Solubility and viscosity of refrigerant-oil mixtures.

ACKNOWLEDGEMENT

The authors would like to thank the member companies of the Air Conditioning and Refrigeration Center at the University of Illinois at Urbana-Champaign for their funding to support this project, Bergstrom for compressor, Sanhua for EEV, and Creative Thermal Solutions for the technical support.